Ultrasensitive colorimetric detection of murine norovirus using NanoZyme aptasensor

Journal:	*Analytical Chemistry*
Manuscript ID	ac-2018-03300b.R1
Manuscript Type:	Article
Date Submitted by the Author:	17-Oct-2018
Complete List of Authors:	Weerathunge, Pabudi; RMIT University, NanoBiotechnology Research Laboratory, School of Science Ramanathan, Rajesh; RMIT University, NanoBiotechnology Research Laboratory, School of Science Torok, Valeria; South Australian Research and Development Institute, Food Safety and Innovation Hodgson, Kate; South Australian Research and Development Institute Xu, Yun; University of Manchester, School of Chemistry Goodacre, Royston; University of Manchester, Manchester Interdisciplinary Biocentre Behera, Bijay; ICAR-Central Inland Fisheries Research Institute Bansal, Vipul; RMIT University, Sir Ian Potter NanoBioSensing Facility, School of Science

Ultrasensitive colorimetric detection of murine norovirus using NanoZyme aptasensor

Pabudi Weerathunge,[a,‡] Rajesh Ramanathan,[a,‡,*] Valeria A. Torok,[b] Kate Hodgson,[b] Yun Xu,[c] Royston Goodacre,[c] Bijay Kumar Behera,[d] and Vipul Bansal[a,*]

[a]Ian Potter NanoBioSensing Facility, NanoBiotechnology Research Laboratory (NBRL), School of Science, RMIT University, GPO Box 2476, Melbourne VIC 3000, Australia.

[b]South Australian Research and Development Institute (SARDI), Food Safety and Innovation, GPO Box 397, Adelaide, SA 5064, Australia.

[c]School of Chemistry, Manchester Institute of Biotechnology, The University of Manchester, 131 Princess Street, Manchester M1 7DN, UK.

[d]ICAR-Central Inland Fisheries Research Institute, Barrackpore, Kolkata 700100, India.

ABSTRACT: Human norovirus (NoV) remains the most common cause of viral gastroenteritis and the leading cause of viral foodborne outbreaks globally. NoV is highly pathogenic with an estimated median viral infective dose (ID50) ranging from 18 to 1,015 genome copies. For NoV detection, the only reliable and sensitive method available for detection and quantification is RTqPCR. NoV detection in food is particularly challenging, requiring matrix specific concentration of the virus and removal of inhibitory compounds to detection assays. Hence, the RTqPCR method poses some challenges for rapid in-field or point-of-care diagnostic applications. We propose a new colorimetric NanoZyme aptasensor strategy for rapid (10 min) and ultrasensitive (calculated LoD of 3 viruses per assay equivalent to 30 viruses/mL of sample and experimentally-demonstrated LoD of 20 viruses per assay equivalent to 200 viruses/mL) detection of the infective murine norovirus (MNV), a readily-cultivable surrogate for NoV. Our approach combines the enzyme-mimic catalytic activity of gold nanoparticles with high target specificity of an MNV aptamer to create sensor probes that produce a blue colour in the presence of this norovirus, such that the colour intensity provides the virus concentrations. Overall, our strategy offers the most sensitive detection of norovirus or a norovirus surrogate achieved to date using a biosensor approach, enabling for the first time, the detection of MNV virion corresponding to the lower end of the ID_{50} for NoV. We further demonstrate the robustness of the norovirus NanoZyme aptasensor by testing its performance in the presence of other non-target microorganisms, human serum and shellfish homogenate, supporting the potential of detecting norovirus in complex matrices. This new assay format can, therefore, be of significant importance as it allows ultrasensitive norovirus detection rapidly within minutes, while also offering the simplicity of use and need for non-specialized laboratory infrastructure.

Norovirus (NoV) belongs to a genetically diverse group of small, icosahedral, non-enveloped viruses with a positive sense single-stranded RNA (ssRNA) genome.[1-2] They are the members of the family *Caliciviridae* and are the major cause of acute viral gastroenteritis worldwide, commonly known as "winter vomiting disease".[1-2] NoV is highly contagious due to its low infective dose (median infective dose, ID_{50} estimated at 18 to 1,015 genome copies),[3] prolonged period of viral shedding, asymptomatic infection in some individuals, high reoccurrence rate and high stability within the environment; posing major challenges in NoV management.[1] NoV is primarily spread through person-to-person contact, as well as, through consumption of contaminated food or water, aerosolised vomit particles or contact with contaminated surfaces. NoV is estimated to account for 267 million infections and over 200,000 deaths (particularly in the young, elderly and immunosuppressed patients) per year,[4-5] with outbreaks often occurring in semi-closed communities such as schools, nursing homes, hospitals and cruise ships.[6] Foods can become contaminated *via* contact with contaminated water, poor hygiene and food handlers, with foods of highest risk being raw shellfish, berries and ready-to-eat foods. Furthermore, the open cross-border trade policies of food products promote global outbreaks.[7-10] Collectively, these highlight the need for a rapid and accurate detection strategy for this important human and foodborne pathogen.

The current gold standard for NoV detection and quantification is based on gene amplification techniques such as reverse transcription quantitative polymerase chain reaction (RTqPCR),[4-5] although a number of alternative methods for NoV detection have been reported (Table 1).[1-2, 7, 11] To our knowledge, the most sensitive alternative NoV detection system reported till date is based on an electrochemical aptasensor approach, wherein the binding of

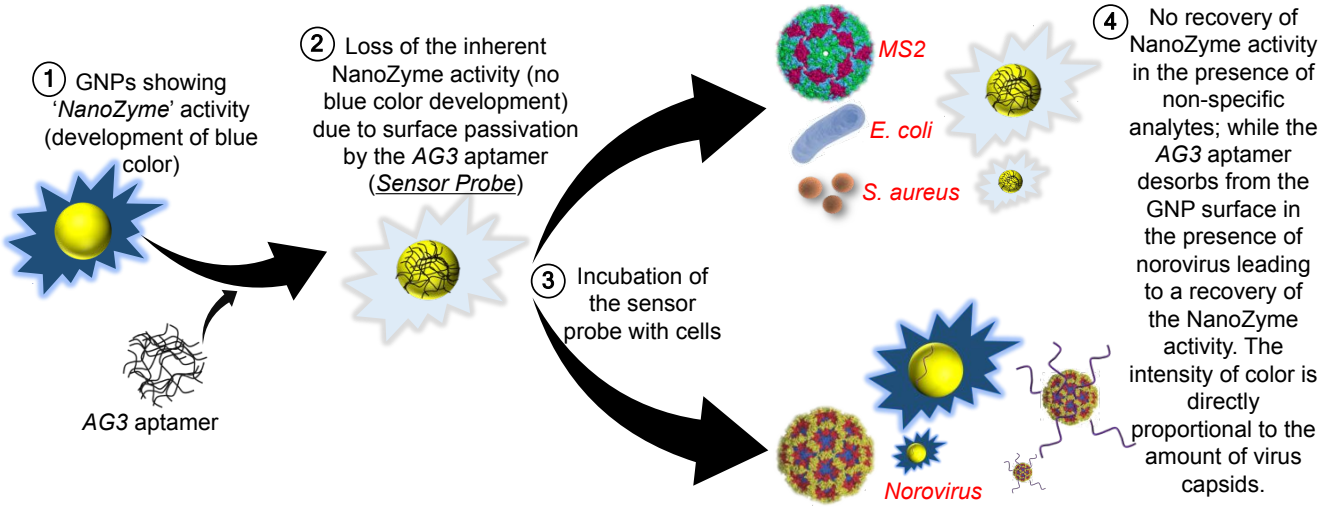

Scheme 1. **Working principle of the norovirus NanoZyme aptasensor**. Schematic illustration outlining the steps involved during norovirus sensing. **Step 1** shows the NanoZyme activity of GNPs that converts a colourless TMB substrate to a blue oxidized product. **Step 2** involves the non-covalent adsorption of the MNV-specific *AG3* aptamer molecules on to the surface of GNPs leading to the loss of the inherent NanoZyme activity. This GNP-aptamer conjugate serves as the '*Sensor Probe*'. **Step 3** involves the incubation of the sensor probe with different cells, including murine norovirus (specific target), *MS2* phage (structurally similar to norovirus), *S. aureus* and *E. coli*. **Step 4** shows that in the presence of norovirus, the aptamers desorb from the surface of the GNPs leading to the recovery of the NanoZyme activity, producing a blue colour. The intensity of colour will be proportional to the amount of norovirus present in the sample. In contrast, since aptamers will not have any affinity to other contaminants, no recovery of the NanoZyme activity will be observed, thereby resulting in no colour in the presence of non-specific targets.

norovirus to highly specific DNA aptamers afforded a calculated limit of detection (LoD) of 180 murine norovirus (MNV) particles or 6,000 MNV/mL.[2] While promising, this LoD is still far-off from meeting the lower end of the median viral infective dose (ID_{50}), estimated to range from 18 to 1,015 genome copies.[3] Development of an ultrasensitive, specific, rapid and user-friendly platform for NoV detection would be particularly advantageous for detecting clinical, environmental and food contamination, with a possibility of portable in-field translation.

The developments in nanotechnology have seen the emergence of colorimetric and other potential biosensing platforms as a viable technology for point-of-care devices.[12-27] Gold nanoparticles (GNPs), in particular, have been at the forefront due to well-established synthesis routes, ease of surface functionalisation, high stability, low cost, low toxicity and remarkable surface plasmon resonance (SPR) properties that allow a visual read-out of the sensing event.[28-38] However, GNP-based sensors that rely on colour generation *via* the SPR properties of gold find it rather challenging to avoid aggregation in complex biological fluids, resulting in non-specificity and false positives.[39-42] In recent years, the aggregation-induced non-specificity of GNPs has been overcome by developing GNP-based NanoZyme sensors that do not rely upon the SPR properties, but instead take advantage of the enzyme-mimicking catalytic activity of gold to convert a colourless substrate into a coloured product.[43-48] However, in the absence of a targeting moiety, the applicability of NanoZyme sensors remains limited, as NanoZymes can exhibit broad-spectrum catalytic activities against a range of substrates. More recently, we have been able to add an element of specificity in NanoZyme sensors by incorporating target-specific molecular recognition elements (MREs) to allow colorimetric detection of small molecules such as pesticides and antibiotics.[49-50]

The use of MREs is common in traditional biomolecular detection systems, e.g., antibodies as in enzyme-linked immunosorbent assay (ELISA),[51] unique polynucleotide sequences in PCR,[52] or lectins in lectin-binding assays (LBA).[53] A relatively new class of non-stereotypical MRE that has remarkable potential in providing specificity to biosensors are aptamers.[16, 54] These synthetic nucleic acids fold into unique three-dimensional conformations and are capable of binding to their targets with high specificity and outstanding affinity.[16, 55] The distinguishing feature of aptamers from other MREs is that they can be raised *in silico* against the vast majority of targets ranging from small molecules[49-50] to complex biological entities such as cancer cells,[56-57] pathogenic bacteria[58-59] and viruses.[2, 60] Aptamers are particularly attractive for biosensors development as they also exhibit high ambient storage stability and affordable on-going *in vitro* synthesis cost once the aptamers have been designed for a particular assay.[16, 55, 61]

In the current study, we combine the outstanding target-specificity of a MNV *AG3* aptamer[2] with the NanoZyme activity of GNPs to develop a rapid colorimetric sensor for ultrasensitive and highly specific detection of the MNV virion. The two reasons for using MNV instead of human norovirus (HuNoVs) are: (i) the production of HuNoV involves laborious process[62] and (ii) murine NoV is an infectious easily cultivable human NoV surrogate enabling the infective particles to be accurately quantified using a plaque assay. Such a model allows the developed senor to

be evaluated for accuracy in detecting infective virus particles as opposed to non-infective coat protein or non-

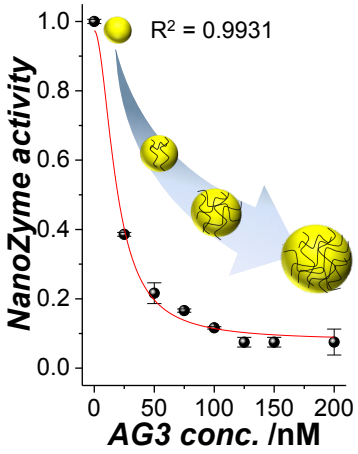

Fig. 1. **Sensor probe fabrication.** Decrease in the NanoZyme activity of the GNPs plotted as a function of *AG3* aptamer concentration. The data was fitted (red curve) using a non-linear least square reverse Hill equation.

encapsidated/damaged viral genome. Neither VLP or NoV strains sourced from human faeces accurately allow for this as quantification is based on total protein concentration or detection of both infective and non-infective viral genomes, respectively. Therefore, the current work utilises murine norovirus (MNV), a cultivable surrogate of NoV as a model system, and demonstrates that the proposed NanoZyme aptasensor technology can detect the infective MNV with a calculated LoD of just 3 viruses in 100 µL sample (equivalent to 30 viruses/mL), the lowest known limit, achieved to date, and that too within a short assay time of only 10 min. We further demonstrate the potential applicability of our Nanozyme aptasensor in the real-world scenario by demonstrating that it retains its functionality in the presence of potential contaminants such as other bacteria and viruses, while being able to reliably detect MNV in complex matrices of human serum and shellfish homogenate. These outcomes offer new opportunities for practical deployment of the norovirus NanoZyme aptasensor for detecting human infections as well as contaminated food.

Scheme 1 illustrates the NanoZyme aptasensor approach for colorimetric detection of norovirus, providing an ultrasensitive and highly specific visual readout of the sensing event within 10 min. The underlying concept is built around utilising the inherent peroxidase-like NanoZyme activity of GNPs to generate a characteristic blue colour through the oxidation of a colourless peroxidase substrate TMB (3,3',5,5'-tetramethylbenzidine) (*Step 1*). Surface passivation of the GNPs with a MNV capsid-specific *AG3* aptamer[2] results in the loss of the colour-generating NanoZyme activity (*Step 2*). This GNP-aptamer nanoconjugate serves as the sensor probe. When this sensor probe is exposed to the analyte (*Step 3*), the NanoZyme activity towards generating blue colour *via* TMB oxidation is selectively recovered in the presence of norovirus, and not in the presence of any other non-specific virus or bacterial cell (*Step 4*). The recovery of the NanoZyme activity in the presence of norovirus is due to the high affinity of *AG3* aptamer towards MNV, which causes conformational changes in the aptamer in the presence of norovirus, leading to their displacement from the GNP surface and binding to the MNV capsid. This aptamer desorption exposes the catalytic sites on the surface of the GNPs to allow TMB oxidation into a blue product. In contrast, in the absence of norovirus, but in the presence of non-specific targets such as Gram-positive bacteria *Staphylococcus aureus*, Gram-negative bacteria *Escherichia coli*, or even a structurally similar virus such as *E. coli* bacteriophage MS2 (MS2 phage), the aptamers do not desorb from the GNP surface and the NanoZyme activity is not recovered, thereby offering selectivity to the sensor.

As the generation of blue colour due to the NanoZyme activity of the GNPs is central to the sensor mechanism, we first established the enzyme-like characteristics of tyrosine-functionalized GNPs (detailed in Supporting Information, **Fig. S1–S4**) synthesized using a previously established protocol (Fig. S1). The GNPs were of low polydispersity, high crystallinity, and of quasi-spherical morphology with an average diameter of *ca*. 20 nm (Fig. S2). The peroxidase-mimic NanoZyme activity of these GNPs shows nanoparticle, TMB and H_2O_2 concentration-dependent increase in activity (Fig. S3), as observed for other NanoZymes.[12, 45-46, 49-50, 63-64] We also calculated the kinetic parameters such as Michaelis-Menten constant (*Km*), maximum initial velocity (*Vmax*) and turnover number (*Kcat*) for the NanoZyme-driven reactions (**Table S1** and Fig. S4). The NanoZyme kinetic parameters suggest that tyrosine-functionalized GNPs offer over three order of magnitude higher affinity to colorigenic TMB substrate in comparison to that to the co-substrate H_2O_2. This is a desirable property in terms of achieving high sensitivity and reproducibility during sensing, as high affinity of NanoZyme towards TMB is likely to allow even low concentrations of target analyte to be identified while using the sensor probe developed in the next stage.

We then developed the sensor probe through binding of MNV-specific *AG3* aptamer to the surface of GNPs. This required determination of the minimum concentration of the *AG3* aptamer needed to passivate the GNP surface without the availability of excessive amounts of free aptamer molecules around the GNP-aptamer nanoconjugates. **Fig. 1** shows that the NanoZyme activity of GNPs decreases with the increasing aptamer concentration, as structural flexibility of aptamers allows them to passivate the GNP surface *via* electrostatic interactions.[65] As such, our calculations reveal that an optimum sensor probe requires an average of ~250 aptamer molecules per GNP to block its NanoZyme activity (see Supporting Information for details). The non-linear least square fitting of the aptamer-GNP interactions revealed a dissociation constant (K_d) of 1.85×10^{-8} M and a Hill coefficient (association stoichiometry) of 1.91. The Hill coefficient value of >1 reflects a positive cooperative binding behaviour, such that the binding of an aptamer molecule to the GNP surface enhances the affinity of other

aptamer molecules to bind to the surface of the NanoZyme (**Table S2**).[66-67] The observed K_d for the aptamer-GNP interactions corroborates well with the previously observed values for stable non-covalently bonded biomolecule-GNP systems.[68] The previous work has shown that the K_d for the *AG3* aptamer to MNV is in the low

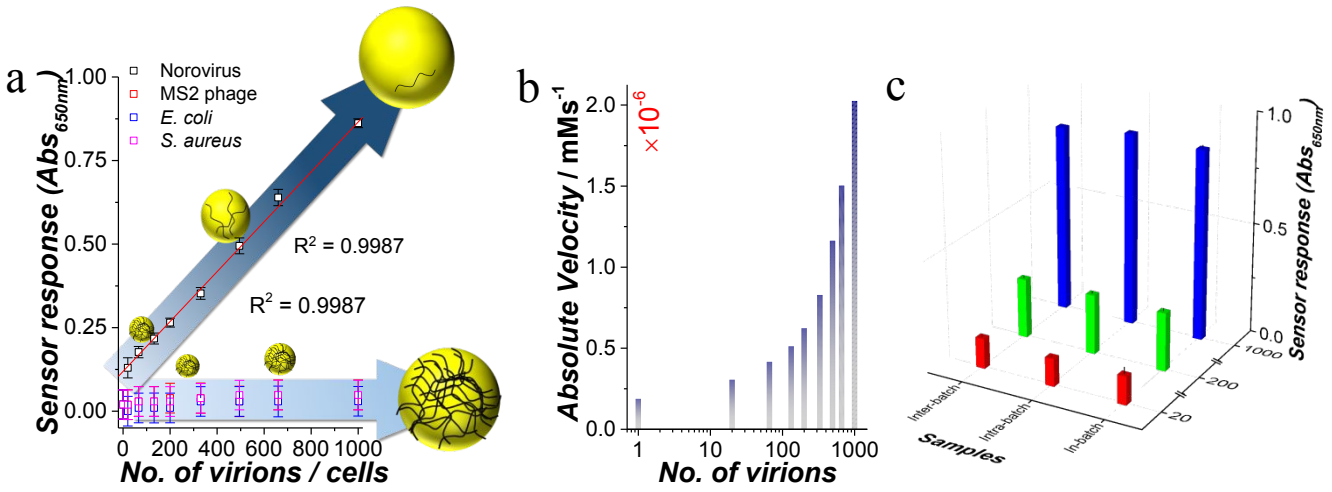

Fig. 2. Sensor response for norovirus detection. (a) The colorimetric sensor response obtained from the incubation of the sensor probe for 10 min with increasing number of different biological entities including MNV, MS2 phage, *S. aureus*, and *E. coli*. The arrows represent the change in the intensity of blue colour formed as a result of aptamer dissociation from the GNP surface leading to the recovery of the NanoZyme activity. The red curve shows the linear fit of the sensor response in the presence of increasing number of norovirus. **(b)** The reaction velocity calculated from the sensor response using enzyme kinetic theory in the absence and presence of increasing number of norovirus. **(c)** In-batch, intra-batch and inter-batch sensor reproducibility for three independent amounts of norovirus (20, 200 and 1,000 viruses) with corresponding precision and accuracy outlined in Table S3, Supporting Information.

picomolar range (10^{-12} M). Conversely, our current work shows the K_d for the *AG3* aptamer to the GNPs is 1.85×10^{-8} M. This suggests that the *AG3* aptamer has almost four orders of magnitude higher binding affinity to MNV than to the GNP. This relative interaction strength of the *AG3* aptamer to MNV *vs.* GNP suggests that when the GNP-aptamer conjugate is exposed to MNV (Step 3, Scheme 1), the aptamers will dissociate from the surface of the GNPs to bind effectively to the target norovirus (Step 4, Scheme 1). Furthermore, the GNP-aptamer nanoconjugates remain stable in solution post-aptamer functionalisation (**Fig. S5**, Supporting Information), and serve as sensor probes for subsequent colorimetric detection of norovirus.

The utility of these NanoZyme aptasensor probes for rapid, sensitive and selective detection of norovirus was assessed by first incubating the sensor probe independently with increasing population of different viruses and bacteria for 10 min. We selected three different biological backgrounds in addition to norovirus, each representing a specific group of microorganisms that may be present as cross-contaminants in the analyte sample containing norovirus. Among these, MNV serves as the target of interest, MS2 phage represents a non-target virus with morphological and surface characteristics resembling noroviruses, *Staphylococcus aureus* represents Gram-positive group of bacteria and *Escherichia coli* represents Gram-negative bacteria (cell preparation outlined in Supporting Information). **Fig. 2a** shows the colorimetric response corresponding to each biological background obtained from the sensor probe in 10 min. It is clear that the NanoZyme activity is recovered specifically in the presence of norovirus, while all other microorganisms including structurally similar MS2 phage show only basal level activity. This highly specific response is attributed to the high affinity of *AG3* aptamers that were specifically raised against the MNV surface. Furthermore, the sensor response (*i.e.*, the intensity of blue colour) increases with the corresponding increase in the number of MNVs, supporting the viability of the proposed approach for norovirus sensing. As such, this norovirus NanoZyme aptasensor shows an outstanding sensitivity along with an impressive linear operating dynamic range of 20-1,000 norovirus detection with high reliability (R^2 = 0.9987) and that too within an assay time of just 10 min.

To understand the underlying factors for this ultrasensitive response, we further calculated the absolute velocity of the sensor probe-induced reaction in the absence and presence of MNVs at the sensing time-point (t = 10 min). Fig. 2b and **Fig. S6** shows that the absolute velocity of the reaction increases linearly with increasing MNV concentration. Remarkably, a 63% increase in the velocity is observed in the presence of as low as 20 MNVs, while 1000 MNVs enhances the TMB oxidation rate by 10.8 times. The calculated limit of detection (LoD) for this assay is 3 MNV, which will correspond to 37% higher reaction velocity relative to that of the sensor probe (based on the regression analysis in Fig. S6). While the current study shows that we can reliably detect 20 MNV experimentally; it is also likely that we can experimentally detect the LoD of 3 MNV through employing robotic systems that can circumvent potential human sampling errors. Furthermore, considering that our assay employs 100 µL

of the original viral sample in a total assay volume of 200 µL, we have experimentally shown that the current NanoZyme aptasensor can reliably detect at least 200 MNV/mL of the original sample. Considering the LoD of 3 MNV per assay, it should therefore be possible to detect a norovirus concentration of 30 MNV/mL in the original sample. This sensitivity is

Table 1. Comparison of norovirus detection parameters among various platforms with emphasis on potential viral load (concentrations per mL) present in test analyte.

Detection Method	Target	Linear Dynamic Range	Calculated Limit of Detection (LoD)	Signal generation time	Ref
Electrochemical	MNV	20 – 120 aM (*ca.* 1.2×10^4 – 7.2×10^4 viruses/mL)	10 aM (*ca.* 6,000 viruses/mL)	60 min	2
Commercial ELISA kit (NV-AD (III), Denka Seiken, Japan)	NoV VLP	Not given	3.8 ng/mL (*ca.* 2.19×10^8 VLP/mL)[b]	Not given	7
Conventional ELISA	NoV VLP	10 – 10^3 ng/mL	10.4 ng/mL (*ca.* 6.00×10^8 VLP/mL)[b]	>12 hours	7
Graphene-GNP Antibody ELISA	NoV VLP	10^2 – 10^7 pg/mL	92.7 pg/mL (*ca.* 5.35×10^6 VLP/mL)[b]	70 min	7
Dot-blotting	NoV	2.7×10^6 – 2.7×10^8 genome copies/mL	2.7×10^6 genome copies/mL	10 min	11
Microfluidics	NoV	1.6×10^5 – 7.9×10^7 genome copies/mL	9.5×10^4 genome copies/mL	60 min	69
NanoZyme aptasensor	MNV	200 – 10,000 viruses/mL[a] OR 1,320 – 19,800 viruses/mL[a] OR 3,300 – 33,000 viruses/mL[a]	30 viruses/mL[a] 50 viruses/mL[a] 80 viruses/mL[a]	10 min	This work

[a]Linear dynamic range of the NanoZyme aptasensor is tunable by changing the sensor probe composition; [b]calculation for conversion of protein concentration to virus like particle (VLP) concentration is provided in Supporting Information.

within the estimated median ID_{50} of NoV (18-1,015 viral genome copies).[3]

Another desirable feature in a sensor is the ability to operate across a large range of target concentrations. However, this remains challenging as beyond a certain target concentration, the sensor response starts to saturate, underestimating the target concentration. We also noticed this limitation in our NanoZyme aptasensor, such that beyond 1,000 MNVs in the assay, the sensor response became non-linear with respect to the number of virions. To overcome

this issue, we investigated the possibility of active modulation of the dynamic operational range of the norovirus NanoZyme aptasensor by changing the concentration of the NanoZyme (GNPs) in our sensor probe. When the concentration of GNPs during GNP-aptamer sensor probe fabrication was changed from 75 µM originally to 100 µM and 150 µM; the linear dynamic range of operation could be actively modulated from 20-1,000 MNV originally to 132-1,980 and 330-3,300 MNV, respectively (**Fig. S7**, Supporting Information). While the norovirus sensors with low detection limits are more desirable, the ability of the NanoZyme sensor to operate in different dynamic ranges will offer design flexibility for future in-field applications.

We further assessed the precision and accuracy of the norovirus sensor operating in the linear dynamic range of 20-1,000 MNV under different conditions at the viral loads of 20, 200 and 1,000 MNV per assay (**Fig. 2c**). The first test involved performing 20 repeat experiments using sensor probes prepared in a single batch (in-batch). Subsequently, intra-batch variations (*i.e.* creating the sensor probe on different days using the GNPs prepared in a single batch) and inter-batch variations (*i.e.* creating the sensor probe using two independently synthesized GNPs) in norovirus sensor response were assessed. In each of these cases, the sensor responded with >95% (95.9-99.3%) precision, >95% (95-100%) accuracy at a significance level of 0.05,

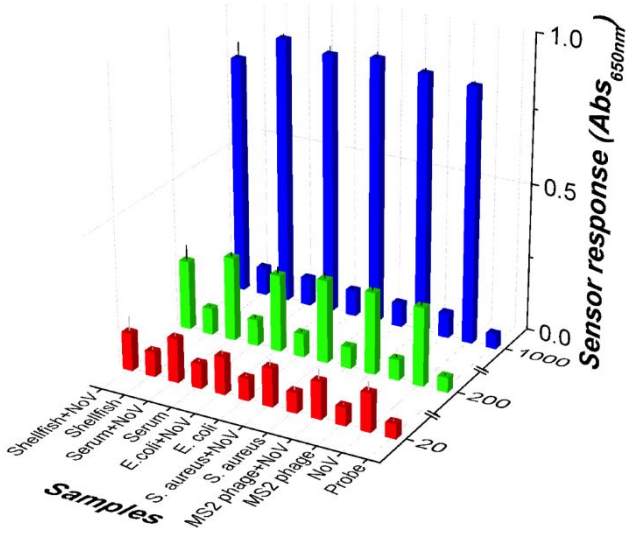

Fig. 3. **Performance of the NanoZyme aptasensor in complex matrices mimicking the real-world scenario.** Sensor response obtained for three independent amounts of norovirus (20, 200 and 1,000) as well as in the absence of norovirus in the presence of a higher population (100,000 cells) of non-specific targets (MS2 phage, *S. aureus*, and *E. coli*); in human serum; and in the shellfish (mussel) homogenate.

and 100% accuracy at a significance level of 0.1 (see **Table S3,** Supporting Information). These observations support the robustness of the NanoZyme aptasensor. The unprecedented sensitivity of the current norovirus sensing platform over previously reported norovirus sensors is summarised in **Table 1**. To allow a valid comparison between different norovirus sensors, the sensor performance data presented in Table 1 has been normalised to virus per mL of the original sample containing norovirus. The most sensitive norovirus detection system reported to date is based on an electrochemical aptasensor that offers a linear dynamic range of 360-2,170 MNV (equivalent of 12,000-72,333 MNV/mL) with a LoD of 6,000 MNV/mL.[2] In comparison, our current sensor shows 200 times higher sensitivity with an absolute LoD of ~3 viruses (30 MNV/mL) along with a tunable linear dynamic detection range that allows detection of 20-3,300 norovirus during the assay, facilitating the viral loads of 200-33,000 norovirus/mL detectable in test analyte. This outlines the outstanding sensitivity and robustness of the current NanoZyme aptasensor technology to selectively detect norovirus. In addition, the simplicity of the current assay and eliminating the need for trained technical personnel can potentially offer a viable option to develop point-of-care norovirus detection devices.

We further evaluated the target-specific performance of the norovirus NanoZyme aptasensor in conditions similar to those encountered during the real-world analysis of a potentially contaminated sample (**Fig. 3** and **Table S3**). These included three different scenarios, the first mimicking a situation where non-specific bacterial and viral loads might be significantly higher (10^5) than norovirus (20, 200 and 1000); the second case considering the potential interference caused by exogenous proteins (human sera); and the third scenario testing the ability of norovirus detection in raw shellfish (mussels) homogenate. The contaminant species present in these scenarios may potentially lead to non-specific response due to sample matrix interference. However, the robustness of the NanoZyme aptasensor supported by the high affinity of *AG3* aptamer towards MNV resulted in excellent recoveries ranging between 96.7-101.8% during norovirus detection in each of these cases, as determined using the linear fit model obtained from Fig. 2b (**Table 2**). This demonstrates the outstanding ability of the current NanoZyme aptasensor technology to selectively detect norovirus even in the presence of other viral and bacterial contaminants, as well as in complex biological matrices.

In summary, we have demonstrated a highly robust NanoZyme aptasensor technology for rapid, highly selective and ultrasensitive colorimetric detection of MNV, a cultivable surrogate of human NoV. The proposed sensing technology combines the outstanding affinity of specific aptamers with the inherent peroxidase-like NanoZyme activity of GNPs to develop a robust platform for norovirus sensing with potential for further point-of-care human diagnostic and in-field food and environmental screening development. This novel technology is the most sensitive norovirus sensor reported to date, which for the first time, demonstrates the ability to detect virus corresponding to a

Table 2. The norovirus recovery obtained from the NanoZyme aptasensor in the presence of different contaminants.

Contaminant	Actual number of norovirus	Recovery[(a)] [%]
MS2 phage	20	99.6
	200	100.9
	1000	100.6
S. aureus	20	99.8
	200	101.2
	1000	101.7
E. coli	20	99.8
	200	99.6
	1000	100.8
Human serum	20	101.8
	200	101.3
	1000	102
Shellfish	20	96.7
	200	97.4
	1000	96.8

[(a)]100% recovery corresponds to expected norovirus numbers, whereas shifts towards lower/ higher values

represent relative under-estimation/ over-estimation of viral loads during norovirus quantification.

low infective dose. The potential of this colorimetric technology in eliminating the need for expensive instrumentation and trained specialized technical personnel may allow in-field translation as a point-of-care NoV diagnostic device.

ASSOCIATED CONTENT

Supporting Information

The Supporting Information is available free of charge on the ACS Publications website.

Details of chemicals, experiments, instruments, materials characterization, and sensor performance evaluation (PDF)

AUTHOR INFORMATION

Corresponding Author

*rajesh.ramanathan@rmit.edu.au; vipul.bansal@rmit.edu.au

Author Contributions

The manuscript was written through contributions of all authors. ‡These authors contributed equally.

ACKNOWLEDGMENT

This work was supported through an Australian Research Council (ARC) Future Fellowship to V. Bansal (FT140101285). V. Bansal and R. Ramanathan acknowledge the ARC for funding support through the ARC Discovery scheme (DP170103477). R. Ramanathan acknowledges RMIT University for the Vice Chancellor Fellowship. B. K. Behera thanks the Commonwealth of Australia for an Endeavour Research Fellowship. The authors acknowledge the generous support of the Ian Potter Foundation for establishing Sir Ian Potter NanoBioSensing Facility at RMIT University. The authors also acknowledge the support from the RMIT Microscopy and Microanalysis Facility (RMMF) for technical assistance and providing access to characterization facilities. Support from the Australian Seafood CRC and Fisheries Research and Development Corporation are also acknowledged (FRDC 2011/726).

REFERENCES

1. Patel, M. M.; Hall, A. J.; Vinjé, J.; Parashar, U. D., Noroviruses: a comprehensive review. *J. Clin. Virol.* **2009,** *44*, 1-8.
2. Giamberardino, A.; Labib, M.; Hassan, E. M.; Tetro, J. A.; Springthorpe, S.; Sattar, S. A.; Berezovski, M. V.; DeRosa, M. C., Ultrasensitive norovirus detection using DNA aptasensor technology. *PLoS One.* **2013**, e79087.
3. Teunis, P. F. M.; Moe, C. L.; Liu, P.; E. Miller, S.; Lindesmith, L.; Baric, R. S.; Le Pendu, J.; Calderon, R. L., Norwalk virus: How infectious is it? *J. Med. Virol.* **2008,** *80*, 1468-1476.
4. Lopman, B.; Atmar, R.; Baric, R.; Estes, M.; Hall, A.; Iturriza-Gómara, M.; Kang, C.; Lee, B.; Parashar, U.; Riddle, M.; Vinjé, J. *Global burden of norovirus and prospects for vaccine development*; Global burden of norovirus and prospects for vaccine development, CDC Foundation Global Burden Report: 2015; pp 1-44.
5. Lopman, B. A.; Steele, D.; Kirkwood, C. D.; Parashar, U. D., The vast and varied global burden of norovirus: prospects for prevention and control. *PLoS Med.* **2016,** *13*, e1001999.
6. Debbink, K.; Lindesmith, L. C.; Donaldson, E. F.; Baric, R. S., Norovirus immunity and the great escape. *PLoS Pathog.* **2012,** *8*, e1002921.
7. Ahmed, S. R.; Takemeura, K.; Li, T.-C.; Kitamoto, N.; Tanaka, T.; Suzuki, T.; Park, E. Y., Size-controlled preparation of peroxidase-like graphene-gold nanoparticle hybrids for the visible detection of norovirus-like particles. *Biosens. Bioelectron.* **2016,** *87*, 558-565.
8. Hagström, A. E.; Garvey, G.; Paterson, A. S.; Dhamane, S.; Adhikari, M.; Estes, M. K.; Strych, U.; Kourentzi, K.; Atmar, R. L.; Willson, R. C., Sensitive detection of norovirus using phage nanoparticle reporters in lateral-flow assay. *PLoS One* **2015**.
9. Gould, L. H.; Kline, J.; Monahan, C.; Vierk, K., Outbreaks of disease associated with food imported into the United States, 1996–2014. *Emerg. Infect. Dis.* **2017,** *23*, 525-528.
10. Holley, R. A., Food safety challenges within North American free trade agreement (NAFTA) partners. *Compr. Rev. Food Sci. Food Saf.* **2011,** *10*, 131-142.
11. Kim, J.-H.; Park, J.-E.; Lin, M.; Kim, S.; Kim, G.-H.; Park, S.; Ko, G.; Nam, J.-M., Sensitive, Quantitative Naked-Eye Biodetection with Polyhedral Cu Nanoshells. *Adv. Mater.* **2017,** *29*, 1702945-n/a.
12. Karim, M. N.; Anderson, S. R.; Singh, S.; Ramanathan, R.; Bansal, V., Nanostructured silver fabric as a free-standing NanoZyme for colorimetric detection of glucose in urine. *Biosens. Bioelectron.* **2018,** *110*, 8-15.
13. Daniel, M. C.; Astruc, D., Gold nanoparticles: assembly, supramolecular chemistry, quantum-size-related properties, and applications toward biology, catalysis, and nanotechnology. *Chem. Rev.* **2004,** *104*, 293-346.
14. Saha, K.; Agasti, S. S.; Kim, C.; Li, X.; Rotello, V. M., Gold nanoparticles in chemical and biological sensing. *Chem. Rev.* **2012,** *112*, 2739-2779.
15. Miranda, O. R.; Creran, B.; Rotello, V. M., Array-based sensing with nanoparticles: "Chemical noses" for sensing biomolecules and cell surfaces. *Curr. Opin. Chem. Biol.* **2010,** *14*, 728-736.
16. Sharma, T. K.; Ramanathan, R.; Rakwal, R.; Agrawal, G. K.; Bansal, V., Moving forward in plant food safety and security through NanoBioSensors: Adopt or adapt biomedical technologies? *Proteomics* **2015,** *15*, 1680-1692.
17. Walia, S.; Sabri, Y.; Ahmed, T.; Field, M. R.; Ramanathan, R.; Arash, A.; Bhargava, S. K.; Sriram, S.; Bhaskaran, M.; Bansal, V., Defining the role of humidity in the ambient degradation of few-layer black phosphorus. *2D Mater.* **2016,** *4*, 015025.
18. Ramanathan, R.; Walia, S.; Kandjani, A. E.; Balendran, S.; Mohammadtaheri, M.; Bhargava, S. K.; Kalantar-zadeh, K.; Bansal, V., Low-temperature fabrication of alkali metal–organic charge transfer complexes on cotton textile for optoelectronics and gas sensing. *Langmuir* **2015,** *31*, 1581-1587.
19. Ramanathan, R.; Kandjani, A. E.; Walia, S.; Balendhran, S.; Bhargava, S. K.; Kalantar-zadeh, K.; Bansal, V., 3-D nanorod arrays of metal-organic KTCNQ semiconductor on textiles for flexible organic electronics. *RSC Adv.* **2013,** *3*, 17654-17658.
20. De La Rica, R.; Stevens, M. M., Plasmonic ELISA for the ultrasensitive detection of disease biomarkers with the naked eye. *Nature Nanotech.* **2012,** *7*, 821.
21. Rodríguez-Lorenzo, L.; De La Rica, R.; Álvarez-Puebla, R. A.; Liz-Marzán, L. M.; Stevens, M. M., Plasmonic nanosensors with inverse sensitivity by means of enzyme-guided crystal growth. *Nat. Mater.* **2012,** *11*, 604.
22. Le, N. D. B.; Yesilbag Tonga, G.; Mout, R.; Kim, S.-T.; Wille, M. E.; Rana, S.; Dunphy, K. A.; Jerry, D. J.; Yazdani, M.; Ramanathan, R.; Rotello, C. M.; Rotello, V. M., Cancer Cell Discrimination Using Host–Guest "Doubled" Arrays. *J. Am. Chem. Soc.* **2017,** *139*, 8008-8012.

23. Rezk, A. R.; Walia, S.; Ramanathan, R.; Nili, H.; Ou, J. Z.; Bansal, V.; Friend, J. R.; Bhaskaran, M.; Yeo, L. Y.; Sriram, S., Acoustic–Excitonic Coupling for Dynamic Photoluminescence Manipulation of Quasi-2D MoS2 Nanoflakes. *Adv. Optical Mater.* **2015,** *3*, 888-894.
24. Behera, B. K.; Das, A.; Sarkar, D. J.; Weerathunge, P.; Parida, P. K.; Das, B. K.; Thavamani, P.; Ramanathan, R.; Bansal, V., Polycyclic Aromatic Hydrocarbons (PAHs) in inland aquatic ecosystems: Perils and remedies through biosensors and bioremediation. *Environ. Poll.* **2018,** *241*, 212-233.
25. Zou, W.; González, A.; Jampaiah, D.; Ramanathan, R.; Taha, M.; Walia, S.; Sriram, S.; Bhaskaran, M.; Dominguez-Vera, J. M.; Bansal, V., Skin color-specific and spectrally-selective naked-eye dosimetry of UVA, B and C radiations. *Nat. Commun.* **2018,** *9*, 3743.
26. Selvakannan, P.; Ramanathan, R.; Plowman, B. J.; Sabri, Y. M.; Daima, H. K.; O'Mullane, A. P.; Bansal, V.; Bhargava, S. K., Probing the effect of charge transfer enhancement in off resonance mode SERS via conjugation of the probe dye between silver nanoparticles and metal substrates. *Phys. Chem. Chem. Phys.* **2013,** *15*, 12920-12929.
27. Chen, F.; Tang, F.; Yang, C.-T.; Zhao, X.; Wang, J.; Thierry, B.; Bansal, V.; Dai, J.; Zhou, X., Fast and Highly Sensitive Detection of Pathogens Wreathed with Magnetic Nanoparticles Using Dark-Field Microscopy. *ACS Sens.* **2018**, DOI: 10.1021/acssensors.8b00785.
28. Muhamadali, H.; Subaihi, A.; Mohammadtaheri, M.; Xu, Y.; Ellis, D. I.; Ramanathan, R.; Bansal, V.; Goodacre, R., Rapid, accurate, and comparative differentiation of clinically and industrially relevant microorganisms via multiple vibrational spectroscopic fingerprinting. *Analyst* **2016,** *141*, 5127-5136.
29. Boisselier, E.; Astruc, D., Gold nanoparticles in nanomedicine: preparations, imaging, diagnostics, therapies and toxicity. *Chem. Soc. Rev.* **2009,** *38*, 1759-1782.
30. Zohora, N.; Kumar, D.; Yazdani, M.; Rotello, V. M.; Ramanathan, R.; Bansal, V., Rapid colorimetric detection of mercury using biosynthesized gold nanoparticles. *Colloid Surf. A.* **2017,** *532*, 451-457.
31. Zayats, M.; Baron, R.; Popov, I.; Willner, I., Biocatalytic growth of Au nanoparticles: from mechanistic aspects to biosensors design. *Nano Lett.* **2005,** *5*, 21-25.
32. Carnovale, C.; Bryant, G.; Shukla, R.; Bansal, V., Size, shape and surface chemistry of nano-gold dictate its cellular interactions, uptake and toxicity. *Prog. Mater Sci.* **2016,** *83*, 152-190.
33. Sabri, Y. M.; Ippolito, S. J.; Tardio, J.; Bansal, V.; O'Mullane, A. P.; Bhargava, S. K., Gold nanospikes based microsensor as a highly accurate mercury emission monitoring system. *Sci. Rep.* **2014,** *4*, 6741.
34. Kim, J. E.; Choi, J. H.; Colas, M.; Kim, D. H.; Lee, H., Gold-based hybrid nanomaterials for biosensing and molecular diagnostic applications. *Biosens. Bioelectron.* **2016,** *80*, 543-559.
35. Mohammadzadeh-Asl, S.; Keshtkar, A.; Ezzati Nazhad Dolatabadi, J.; de la Guardia, M., Nanomaterials and phase sensitive based signal enhancment in surface plasmon resonance. *Biosens. Bioelectron.* **2018,** *110*, 118-131.
36. Syedmoradi, L.; Daneshpour, M.; Alvandipour, M.; Gomez, F. A.; Hajghassem, H.; Omidfar, K., Point of care testing: The impact of nanotechnology. *Biosens. Bioelectron.* **2017,** *87*, 373-387.
37. Reguera, J.; Langer, J.; Jiménez De Aberasturi, D.; Liz-Marzán, L. M., Anisotropic metal nanoparticles for surface enhanced Raman scattering. *Chem. Soc. Rev.* **2017,** *46*, 3866-3885.
38. Anderson, S. R.; Mohammadtaheri, M.; Kumar, D.; O'Mullane, A. P.; Field, M. R.; Ramanathan, R.; Bansal, V., Robust nanostructured silver and copper fabrics with localized surface plasmon resonance property for effective visible light induced reductive catalysis. *Adv. Mater. Interfaces* **2016,** *3*, 1500632.
39. Vilela, D.; González, M. C.; Escarpa, A., Sensing colorimetric approaches based on gold and silver nanoparticles aggregation: chemical creativity behind the assay. A review. *Anal. Chim. Acta* **2012,** *751*, 24-43.
40. Jv, Y.; Li, B.; Cao, R., Positively-charged gold nanoparticles as peroxidiase mimic and their application in hydrogen peroxide and glucose detection. *Chem. Commun.* **2010,** *46*, 8017-8019.
41. Long, Y. J.; Li, Y. F.; Liu, Y.; Zheng, J. J.; Tang, J.; Huang, C. Z., Visual observation of the mercury-stimulated peroxidase mimetic activity of gold nanoparticles. *Chem. Commun.* **2011,** *47*, 11939-11941.
42. Guo, L.; Xu, Y.; Ferhan, A. R.; Chen, G.; Kim, D.-H., Oriented gold nanoparticle aggregation for colorimetric sensors with surprisingly high analytical figures of merit. *J. Am. Chem. Soc.* **2013,** *135*, 12338-12345.
43. Lin, Y.; Ren, J.; Qu, X., Catalytically active nanomaterials: a promising candidate for artificial enzymes. *Acc. Chem. Res.* **2014,** *47*, 1097-1105.
44. Weerathunge, P.; Sharma, T. K.; Ramanathan, R.; Bansal, V., Nanozyme-Based Environmental Monitoring. In *Advanced Environmental Analysis: Applications of Nanomaterials*, The Royal Society of Chemistry: 2017; Vol. 2, pp 108-132.
45. Wei, H.; Wang, E., Nanomaterials with enzyme-like characteristics (nanozymes): next-generation artificial enzymes. *Chem. Soc. Rev.* **2013,** *42*, 6060-6093.
46. Wang, X.; Hu, Y.; Wei, H., Nanozymes in bionanotechnology: from sensing to therapeutics and beyond. *Inorg. Chem. Front.* **2016,** *3*, 41-60.
47. Tonga, G. Y.; Jeong, Y.; Duncan, B.; Mizuhara, T.; Mout, R.; Das, R.; Kim, S. T.; Yeh, Y.-C.; Yan, B.; Hou, S.; Rotello, V. M., Supramolecular regulation of bioorthogonal catalysis in cells using nanoparticle-embedded transition metal catalysts. *Nat. Chem.* **2015,** *7*, 597-603.
48. de la Rica, R.; Stevens, M. M., Plasmonic ELISA for the ultrasensitive detection of disease biomarkers with the naked eye. *Nat. Nanotech.* **2012,** *7*, 821-824.
49. Weerathunge, P.; Ramanathan, R.; Shukla, R.; Sharma, T. K.; Bansal, V., Aptamer-controlled reversible inhibition of gold nanozyme activity for pesticide sensing. *Anal. Chem.* **2014,** *86*, 11937-11941.
50. Sharma, T. K.; Ramanathan, R.; Weerathunge, P.; Mohammadtaheri, M.; Daima, H. K.; Shukla, R.; Bansal, V., Aptamer-mediated 'turn-off/turn-on' nanozyme activity of gold nanoparticles for kanamycin detection. *Chem. Commun.* **2014,** *50*, 15856-15859.
51. Byrne, B.; Stack, E.; Gilmartin, N.; O'Kennedy, R., Antibody-based sensors: Principles, problems and potential for detection of pathogens and associated toxins. *Sensors* **2009,** *9*, 4407-4445.
52. Kovárová, M.; Dráber, P., New specificity and yield enhancer of polymerase chain reactions. *Nucleic Acids Res.* **2000,** *28*, e70-e70.
53. Zhao, J.; Patwa, T. H.; Qiu, W.; Shedden, K.; Hinderer, R.; Misek, D. E.; Anderson, M. A.; Simeone, D. M.; Lubman, D. M., Glycoprotein Microarrays with Multi-Lectin Detection: Unique Lectin Binding Patterns as a Tool for Classifying Normal, Chronic Pancreatitis and Pancreatic Cancer Sera. *J. Proteome Res.* **2007,** *6*, 1864-1874.
54. Dhiman, A.; Kalra, P.; Bansal, V.; Bruno, J. G.; Sharma, T. K., Aptamer-based point-of-care diagnostic platforms. *Sens. Actuators B.* **2017,** *246*, 535-553.
55. Keefe, A. D.; Pai, S.; Ellington, A., Aptamers as therapeutics. *Nat. Rev. Drug Discov.* **2010,** *9*, 537-550.
56. Hung, L.-Y.; Wang, C.-H.; Che, Y.-J.; Fu, C.-Y.; Chang, H.-Y.; Wang, K.; Lee, G.-B., Screening of aptamers specific to colorectal cancer cells and stem cells by utilizing On-chip Cell-SELEX. *Sci. Rep.* **2015,** *5*.
57. Wu, X.; Chen, J.; Wu, M.; Zhao, J. X., Aptamers: active targeting ligands for cancer diagnosis and therapy. *Theranostics* **2015,** *5*, 322.
58. Chang, Y.-C.; Yang, C.-Y.; Sun, R.-L.; Cheng, Y.-F.; Kao, W.-C.; Yang, P.-C., Rapid single cell detection of Staphylococcus aureus

by aptamer-conjugated gold nanoparticles. *Sci. Rep.* **2013,** *3*, 1863.
59. Yang, M.; Peng, Z.; Ning, Y.; Chen, Y.; Zhou, Q.; Deng, L., Highly specific and cost-efficient detection of *Salmonella Paratyphi* A combining aptamers with single-walled carbon nanotubes. *Sensors* **2013,** *13*, 6865-6881.
60. Park, J.-W.; Lee, S. J.; Choi, E.-J.; Kim, J.; Song, J.-Y.; Gu, M. B., An ultra-sensitive detection of a whole virus using dual aptamers developed by immobilization-free screening. *Biosens. Bioelectron.* **2014,** *51*, 324-329.
61. Ruscito, A.; DeRosa, M. C., Small-Molecule Binding Aptamers: Selection Strategies, Characterization, and Applications. *Front. Chem.* **2016,** *4*.
62. Ettayebi, K.; Crawford, S. E.; Murakami, K.; Broughman, J. R.; Karandikar, U.; Tenge, V. R.; Neill, F. H.; Blutt, S. E.; Zeng, X.-L.; Qu, L.; Kou, B.; Opekun, A. R.; Burrin, D.; Graham, D. Y.; Ramani, S.; Atmar, R. L.; Estes, M. K., Replication of human noroviruses in stem cell–derived human enteroids. *Science* **2016,** *353*, 1387-1393.
63. Singh, M.; Weerathunge, P.; Liyanage, P. D.; Mayes, E.; Ramanathan, R.; Bansal, V., Competitive Inhibition of the Enzyme-Mimic Activity of Gd-Based Nanorods toward Highly Specific Colorimetric Sensing of l-Cysteine. *Langmuir* **2017,** *33*, 10006-10015.
64. Karim, M. N.; Singh, M.; Weerathunge, P.; Bian, P.; Zheng, R.; Dekiwadia, C.; Ahmed, T.; Walia, S.; Della Gaspera, E.; Singh, S.; Ramanathan, R.; Bansal, V., Visible-Light-Triggered Reactive-Oxygen-Species-Mediated Antibacterial Activity of Peroxidase-Mimic CuO Nanorods. *ACS Appl. Nano Mater.* **2018,** *1*, 1694-1704.
65. Li, H.; Rothberg, L., Colorimetric detection of DNA sequences based on electrostatic interactions with unmodified gold nanoparticles. *Proc. Natl. Acad. Sci. USA* **2004,** *101*, 14036-14039.
66. Hulme, E. C.; Trevethick, M. A., Ligand binding assays at equilibrium: validation and interpretation. *Brit. J. Pharmacol.* **2010,** *161*, 1219-1237.
67. Dahan, D. S.; Dibas, M. I.; Petersson, E. J.; Auyeung, V. C.; Chanda, B.; Bezanilla, F.; Dougherty, D. A.; Lester, H. A., A fluorophore attached to nicotinic acetylcholine receptor βM2 detects productive binding of agonist to the αδ site. *Proc. Natl. Acad. Sci. USA* **2004,** *101*, 10195-10200.
68. Rana, S.; Le, N. D. B.; Mout, R.; Saha, K.; Gulen, Y. T.; Bain, R. E. S.; Miranda, O. R.; Rotello, C. M.; Rotello, V. M., A multichannel nanosensor for instantaneous readout of cancer drug mechanisms. *Nat. Nanotech.* **2014,** *10*, 65-69.
69. Han, K. N.; Choi, J.-S.; Kwon, J., Three-dimensional paper-based slip device for one-step point-of-care testing. *Sci. Rep.* **2016,** *6*, 25710.

TOC Graphics.